Simplified Extense Source Model for Photoreactor Analysis and Design

Horacio A. Irazoqui,*,† Miguel A. Isla,† and Alberto E. Cassano†

INTEC (Instituto de Desarrollo Tecnológico para la Industria Química), Universidad Nacional del Litoral and CONICET, Güemes 3450, 3000 Santa Fe, Argentina

Most of the research work on photoreactor analysis, modeling, and design published so far relies on two approaches to represent the emission of tubular radiation sources: the line (linear) source models (LSMs) and the extense (three-dimensional) source models (ESMs). It is widely recognized that the ESMs give the more realistic representation of the emission phenomenon so far; however, they are rather difficult to use in some applications, especially when indirect radiation plays a dominant role. On the other hand, LSMs are simpler, and in some cases, mostly when reflected radiation has not been involved, they have been used with success. In this work, the simplified extense model (SEM), systematically derived from the extense source model with voluminal emission (ESVE), is proposed. The SEM retains all of the simplicity of the LSM for the prediction of the direct radiation contribution, while rendering closed mathematical expressions that give a more realistic and often very accurate representation of the reflected radiation inside reflecting cylindrical cavities with elliptical cross sections. The average incident radiation on the reactor surface at the midreactor length as predicted with the SEM never differs by more than 12% of the average value computed with the ESVE. Moreover, for different sets of frequently used parameter values characterizing the shape of the elliptical mirror and the reactor, the compared average values agreed within 5% of the reference value given by the ESVE. Within the same parameter range and for eccentricities of about $e = 0.4$, nonaveraged values of the incident radiation computed at different points on the external surface of the reactor wall at the midreactor height position using the SEM and the ESVE models agreed remarkably well, to the point that, under certain circumstances, the profiles obtained are not easily distinguishable from one another. The SEM brings together simplicity of implementation with desirable accuracy for a wide set of values of the apparatus parameters used to illustrate the proposal.

I. Introduction

The radiation field models of photochemical reactors inside cylindrical reflectors of elliptical cross section have evolved driven by the necessities of accuracy and simplicity. Early incidence[1] and emission[2] models were based on the assumption that beams diverge radially from a linear source on parallel planes perpendicular to the lamp axis, to finally converge after reflection at the reactor on planes that mutually intercept at the reactor center line.

Although attractively simple, parallel-plane incidence or emission models will not be included in this analysis because they do not predict experimental data within an acceptable error, except for special cases (subjected to strong geometrical restrictions) and for cases in which photoreactors are directly irradiated from the lamp.[3] In fact, when the light source is a lamp, incidence models are no longer used for the analysis of photoreactors because it was recognized that the radiative part of the problem must be treated on the grounds of radiative transfer theory and the source, the reflector, and the reactor must be considered as parts of a unique system.

Later, the line source model with spherical and isotropic emission (LSSE model) was presented,[4,5] introducing an approximation that matched reality better than earlier models. The lamp was assumed to be a line made of a succession of point sources emitting isotropically in all directions in space.

As indicated by Alfano et al.,[6] incidence models cannot be used without empirically adjusted parameters. At least one empirical parameter is needed for line models and always more than one in the case of two- or three-dimensional incidence models. In all cases, these parameters depend on the size and geometrical configuration of the reactors. This is a serious drawback for design purposes for it precludes the implementation of systematic scaling-up procedures.

Irazoqui et al.[7] proposed a three-dimensional source model with isotropic and voluminal emission for the first time: the extense source model with voluminal emission (ESVE model), including all of the characteristics of an arc lamp. The lamp model includes all its geometrical dimensions, and it is assumed that each differential volume in the uniform lamp arc emits radiation isotropically in all directions. Later, Stramigioli et al.[8,9] extended the model to lamps with superficial emission (ESSE model).

Line and extense emission models, particularly of the superficial emission type, have also been used with the assumption of diffuse emission. A number of variations and applications have been presented in the literature. The review paper by Alfano et al.[6] offers a comprehensive and critical discussion of this subject.

* Author to whom correspondence should be addressed. Fax: +54 342 455 1917. E-mail: hirazo@alpha.arcride.edu.ar.

† CONICET Research Staff Member and Professor at Universidad Nacional del Litoral.

10.1021/ie9907876 CCC: $19.00
Published on Web 10/07/2000

Three-dimensional source emission models are precise and reliable but are more difficult to implement than two-dimensional models. Despite this fact, they do not present any additional conceptual difficulty because, in both models, all directions across a field point contribute to the local incident energy.

About a decade ago, De Bernardez and Cassano,[10,11] Clariá et al.,[12,13] Alfano et al.,[14−16,19] Alfano and Cassano,[17,18] Esplugas et al.,[20] Vicente et al.,[21] Cabrera et al.,[22−25] and Tymoschuck et al.,[26,27] successfully used source models with both voluminal and superficial emission (the latter being either isotropic or diffuse) in a variety of reactor configurations. Computer times were reasonable, and results agreed quite satisfactorily with bench-scale experimental data, with no experimentally adjustable parameters required.

Romero et al.,[3] in an extensive theoretical work, and De Bernardez and Cassano,[10,11] using theory and experiments, have modeled photoreactors employing the line source model for comparison purposes and when only direct radiation was involved. Annular photoreactors without reflectors were used, and the observed deviations between predicted and measured properties were never larger than 20%. Many authors have successfully used the LSM in laboratory- or bench-scale studies, always considering direct irradiation from the source only.[6] Moreover, Pascuali et al.[28]and Li Puma and Yue[29] have used the LSSE model very recently in annular reactors.

On the basis of experimental evidence, Alfano et al.[14] and Clariá et al.[13] have clearly shown that predictions of radiation field properties using the line models available at the time were far from accurate when ruled curved reflecting surfaces and tubular lamps were part of the emission system, irrespective of whether the mirror was a cylinder of elliptical cross section or a parabola.

When photoreactors with cylindrical reflectors are used, indirect radiation reflected on ruled curved surfaces is an important contribution to the energy density at the reaction zone. Predictions based on the LSSE model have shown discrepancies on the order of 100% in the case of a parabolic reflector[14] and up to 2 orders of magnitude when an elliptical reflector was used[13] when compared with experimental data.

It is evident that the accuracy of the predictions based on line models decreases when the contribution of the reflected radiation, relative to the value of the total incident radiation, increases. In fact, in most of the elliptical reflectors, indirect radiation produces more than 90% of the total incident radiation,[30] whereas in parabolic reflectors, indirect contributions are never larger than 70% of the total.[14]

The problem of reducing complexities arising from the ESVE model is important from many aspects. On one hand, reactors with reflectors have proven to be excellent devices for laboratory- and bench-scale experiments. In the case of elliptical cylinders, they permit: (i) the separation of the lamp from the reactor, facilitating heating or cooling and filtering undesired radiation; (ii) the irradiation of the reactor from the outside, with absorption produced in the opposite direction of the geometrical concentration; and (iii) reactor cross sections compatible with reasonable consumption of reactants in the continuous-operation mode. In the case of parabolic cylinders, in addition to the advantage of having the lamp outside the reactor, they permit good stirring conditions in the reactor vessel and are very suitable for gas−liquid reactions. On the other hand, many photochemical reactions involve complicated mechanisms or reaction sequences with many steps and species. This leads to the existence of several multicomponent mass balance equations that are coupled to each other through their respective reaction rate terms. Moreover, for some species, the reaction rate is coupled to the radiation balance in an unusually difficult fashion because of the local concentration dependence of the radiation absorption coefficient. Additionally, it should be noted that this would be the case for the most favorable situation when thermal effects can be neglected. However, even though from a kinetic point of view thermal effects are generally of a lesser importance in photochemical reactions, the design of the reactor itself (as far as avoiding undesirable thermally activated side reactions or unsafe operating conditions) may require the inclusion of thermal energy balance for the case of highly exothermic reactions. Under these conditions, it would always be advisable to use a radiation source model that, although simple, is as precise as needed.

The aim of the present investigation is the development of a simplified extense model for predicting the radiation field inside an elliptical reflecting cavity with a cylindrical arc lamp source, taking the ESVE as the starting point. The leading notion is that of considering the radiation field properties predicted by the SEM as the respective asymptotic mathematical expressions given by the ESVE in the limit that the lamp radius tends to zero. This process is conceptually different from those considering a line source with spherical emission, which already is the result of a previous physical limiting process, as the starting model element for computing direct and indirect incident radiation at a given point in the reactor resorting to geometrical optics to trace ray trajectories. By operating in this manner, changes in the divergence of the energy beams when reflected on the elliptical mirror are definitely lost, hampering the ability of the LSM to predict radiation contributions (particularly from indirect radiation) with the desired accuracy.

The problem is also important because of the increasing potential applications of concentrated solar energy to many different processes. Curved reflecting surfaces have been one of the most widely used devices for achievement of this photon concentration. Even when the concentrating effect is not sought, compound parabolic collectors make use of reflecting surfaces. Thus, the conclusions obtained in this work can be extended to the case when ruled curved reflecting surfaces are used to improve solar irradiation at the location of cylindrical reactors. These reactors seem to be emerging as an attractive technology for water purification.[31−35] Although solar irradiation is a much more complicated phenomenon than artificial irradiation with lamps, the results of this work will also provide some insights into this problem, particularly in terms of qualitative ideas about some of the starting assumptions for the modeling of different solar reactor configurations.

The approach will be illustrated with the elliptical reflector because this is the reactor arrangement for which existing line models have shown the largest discrepancies. It should be noted that the method can be equally applicable to other reflector geometries, typically the widely used parabolic reflector. The inci-

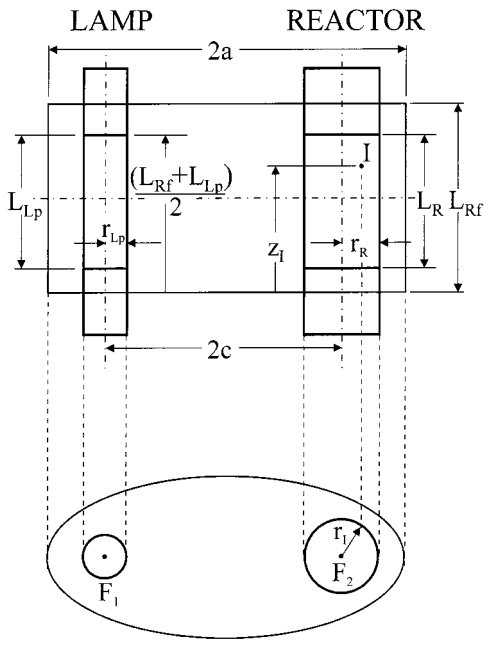

Figure 1. Geometry of the bench-scale setup. Adapted from Cerdá et al.[31]

dent radiation[36] is the field property chosen for comparing the performance of the SEM against that of the ESVE. The latter has been widely considered as the best available model so far for predicting photoreactor radiation field properties, its only important drawback arising from the difficulties of its numerical implementation.

II. Development of the Simplified Extense Model (SEM)

This section will be devoted to the derivation of the simplified extense model (SEM) for predictions of the radiation field inside an elliptical reflecting cavity and a diactinic medium, on the basis of the extense source model with voluminal and isotropic emission (ESVE).[7,30,37] The strategy devised can be applied to other emission models, as is the case with the extense source model with superficial emission.[8,9]

The setup under consideration is made of a cylindrical reflector of elliptical cross section, with one cylindrical, tubular lamp placed at one focal axis and the cylindrical, tubular reactor placed at the other, as shown in Figure 1. The analysis can be extended to the case of a parabolic reflector with a cylindrical lamp collinear with its focal axis irradiating the flat bottom or side of the reactor.

Without loss of generality, the following two simplifying assumptions will be made to reduce the complexity of the mathematical model: (i) only monochromatic radiation will be considered (extensions to polychromatic sources have been precisely treated by Clariá et al.[13]), and (ii) the reactor is assumed to be transparent (a diactinic medium). This means that we are only interested in determining the ability of different lamp−reflector system models to predict the radiation field about the reactor location without the interference of absorption or scattering phenomena. The use of a model with polychromatic and participating media can be implemented in the same way that the ESVE model has been used in the past; however, in this case, the numerical implementation is significantly simpler.

Regarding the ESVE model, we will present here the final equations only. A detailed description of their derivation from model assumptions and of their use in computing the direct and indirect contributions to radiation fields in different setups can be found elsewhere.[7,30,37]

Following Ozisik,[36] the incident radiation is given by

$$G = \int_{4\pi} I \, d\Omega \tag{1}$$

This is the important property in photochemical reactors, for it is related to the local volumetric rate of energy absorption (LVREA), always necessary to express the reaction rate of a kinetically controlled photochemical process, whether it has been derived from a reaction mechanism or from an empirical correlation. The product of the incident radiation times the absorption coefficient of the reactant under consideration gives, at any point inside the reaction space, the LVREA.

II.1. Direct Contribution to the Incident Radiation. *The ESVE Model.* The direct contribution to the incident radiation as predicted with the ESVE[7] model is presented in Appendix AI.1. For a diactinic medium, it simplifies into the expression

$$G_E^D = 2P_V\Psi_R \int_{\phi_1}^{\phi_2} d\phi \, (r_{Lp}^2 - \Delta^2 \sin^2\phi)^{1/2}[\theta_2(\phi) - \theta_1(\phi)] \tag{2}$$

The Simplified Extense Model. We are interested in the asymptotic mathematical expression of eq 2 as the lamp arc radius, r_{Lp}, is continuously contracted to zero, taking on values much smaller than the ellipse parameters a and b.

From the condition that the values of $\rho_{1,2}(\theta,\phi)$ in eq AI.3 be real numbers, it follows that the constraint

$$(r_{Lp}^2 - \Delta^2 \sin^2\phi) \geq 0 \tag{3}$$

must be satisfied as limiting mathematical forms are derived. This condition amounts to say that $(\Delta \sin \phi)$ is an infinitesimal quantity of order greater than or equal to r_{Lp} as $r_{Lp} \to 0$. As a consequence of this, both terms in eq 3 approach their asymptotic forms at least with the same rate. We can conclude that the limiting expression of eq 3 is

$$(r_{Lp}^2 - \Delta^2\phi^2) \geq 0 \quad \text{as } r_{Lp} \to 0 \tag{4}$$

where Δ is a constant and the substitution

$$\sin\phi \approx \phi \quad 0 < \phi < \frac{\pi}{2} \tag{5}$$

valid whenever $\sin \phi \to 0$, has been made. The equality in eq 4 holds for beams with a direction of propagation tangent to the lamp cylindrical body. From eq 4, it can be concluded that the integration limits of eq 2, for $r_{Lp} \to 0$, approach the simpler expressions

$$\phi_2 = \left(\frac{r_{Lp}}{\Delta}\right) \tag{6}$$

and

$$\phi_1 = -\phi_2 \tag{7}$$

respectively.

With the constraint that $(\Delta \sin \phi)$ goes to zero as $r_{Lp} \to 0$ at least as fast as r_{Lp} does, we conclude that the

limit expressions of eq AI.5 and AI.6 are

$$\theta_1 = \tan^{-1}\left[\frac{\Delta}{{}^1/_2(L_{Rf} + L_{Lp}) - z_I}\right] \quad (8)$$

$$\theta_2 = \pi - \tan^{-1}\left[\frac{\Delta}{z_I - {}^1/_2(L_{Rf} - L_{Lp})}\right] \quad (9)$$

where the substitution $\cos\phi \approx 1$ has been made, and where the infinitesimal quantity $(r_{Lp}^2 - \Delta^2 \sin^2\phi)^{1/2}$ has been neglected compared to the constant value Δ. The limit expressions given by eqs 8 and 9 are no longer functions of the integration variable ϕ.

In the limit for $r_{Lp} \to 0$, eq 3 tends to the limit form

$$G_E^D \to 2P_V\Psi_R[\theta_2 - \theta_1]\int_{\phi_1}^{\phi_2} d\phi\,(r_{Lp}^2 - \Delta^2\phi^2)^{1/2} \quad (10)$$

where the integration limits are given by eqs 8 and 9, respectively.

It is shown in Appendix AI.2 that the integration of eq 10 renders an analytical, closed mathematical form.

With the relationship

$$P_L = \pi P_V r_{Lp}^2 \quad (11)$$

where P_L is the lamp constant in the LSSE model given by

$$P_L = \frac{E_{Lp}}{4\pi L_{Lp}} \quad (12)$$

the limit form of eq 3 can be rewritten as

$$G_E^D \to G^D = P_L\Psi_R\frac{[\theta_2 - \theta_1]}{\Delta} \quad (13)$$

From eq 13, we conclude that the asymptotic value of the direct radiation contribution to the incident radiation, G_E^D, given by the SEM coincides with the expression given by the LSSE model.[4,5] This situation will not be found again in the case of the indirect contribution to the incident radiation, because in that case, the two models differ from each other both conceptually and quantitatively.

II.2. Reflected (Indirect) Contribution to the Incident Radiation. *The ESVE Model.* With the assumption that a single reflection is sufficient for the accurate prediction of the indirect contribution to the local radiation field properties in an elliptical cavity at a reception point (r_I, z_I, β_I), we can write[30]

$$G_E^{Rf} = 2P_V\Psi_R\Gamma_{Rf}\int_{\phi_1}^{\phi_2} d\phi\,[r_{Lp}^2 - D^2\sin^2\epsilon(\phi)]^{1/2} \times [\theta_2(\phi) - \theta_1(\phi)] \quad (14)$$

The complete set of equations of the ESVE model for reflected radiation is presented in Appendix AII.1, while the relevant parameters and variables are defined in Figure AII.1.

The Simplified Model. In eq 14, the constraint

$$r_{Lp}^2 \geq D^2\sin^2\epsilon(\phi) \quad (15)$$

must always be satisfied. This condition amounts to the fact that, when the incident ray trajectory is traced backward, the lamp body is intercepted, and consequently, the considered beam contributes to the local incident radiation.

Combining eqs AII.1, AII.2, and AII.3 from Appendix AII.1, we can write

$$D(\phi)\sin\epsilon(\phi) = C[1 + e^2 + 2e\cos(\phi - \epsilon(\phi))]\,r_I\,|\sin(\phi - \beta_I)| \quad (16)$$

where $C = a^2/b^2 > 1$. With these definitions and results, part of the integrand in eq 14 can be rearranged into the following form:

$$r_{Lp}^2 - D^2(\phi)\sin^2\epsilon(\phi) = r_{Lp}^2\left\{1 - C^2[1 + e^2 + 2e\cos(\phi - \epsilon(\phi))]^2\left(\frac{r_I}{r_{Lp}}\right)^2\sin^2(\phi - \beta_I)\right\} \geq 0 \quad (17)$$

which, as will be seen later, is a useful intermediate result.

We will derive asymptotic forms of the equations governing reflected radiation in the limit for $r_{Lp} \to 0$. The constraint of eq 15 must be satisfied as asymptotic mathematical forms are derived. This condition amounts to saying that the product $D(\phi - \epsilon)\sin\epsilon$, where $\epsilon = \epsilon(\phi)$, is an infinitesimal of order greater than or equal to r_{Lp} as $r_{Lp} \to 0$. As a consequence of this, both terms on the lhs of eq 17 approach their asymptotic forms at least with the same rate.

Considering that $D(\phi - \epsilon(\phi))$ always remains finite in the limiting process, we must conclude that, under the constraint of eq 15,

$$\sin\epsilon(\phi) \approx \epsilon(\phi) \to 0 \quad \text{as } r_{Lp} \to 0 \quad (18)$$

up to a first-order approximation of $\sin\epsilon(\phi)$ in terms of its argument $\epsilon(\phi)$.

Considering eqs AII.3 and 18, we conclude that there are two asymptotic forms of eq 17 for $r_{Lp} \to 0$, corresponding to

$$\phi \to \beta_I \quad (19)$$

and

$$\phi \to (\beta_I + \pi) \quad (20)$$

respectively.

In the first case, keeping up to first-order infinitesimals only

$$D(\phi)\sin\epsilon(\phi) \to C[1 + e^2 + 2e\cos(\beta_I)]\,r_I(\phi - \beta_I) \quad \text{as } \phi \to \beta_I \quad (21)$$

while in the second case

$$D(\phi)\sin\epsilon(\phi) \to -C[1 + e^2 - 2e\cos(\beta_I)]\,r_I[\phi - (\beta_I + \pi)] \quad \text{as } \phi \to (\beta_I + \pi) \quad (22)$$

Therefore, the asymptotic form of eq 17 for $\phi \to \beta_I$ is

$$r_{Lp}^2 - D^2(\phi)\sin^2\epsilon(\phi) \to r_{Lp}^2\left\{1 - C^2[1 + e^2 + 2e\cos(\beta_I)]^2\left(\frac{r_I}{r_{Lp}}\right)^2(\phi - \beta_I)^2\right\} \quad (23)$$

while the corresponding form for $\phi \to (\beta_I + \pi)$ is

$$r_{Lp}^2 - D^2(\phi)\sin^2\epsilon(\phi) \rightarrow r_{Lp}^2\left\{1 - C^2[1 + e^2 - 2e\cos(\beta_I)]^2\left(\frac{r_I}{r_{Lp}}\right)^2[\phi - (\beta_I + \pi)]^2\right\} \quad (24)$$

When these results are substituted into eq 17, two contributions to the local indirect incident radiation can be identified, each one having the same general form of eq 12 and therefore being amenable of analytic integration. The results are

$$G_1^{Rf} = \left[\frac{P_L\Psi_R\Gamma_{Rf}}{C}\right]\left\{\frac{1}{[1 + e^2 + 2e\cos(\beta_I)]}[\theta_2^{(1)} - \theta_1^{(1)}]\right\}\frac{1}{r_I} \quad (25)$$

and

$$G_2^{Rf} = \left[\frac{P_L\Psi_R\Gamma_{Rf}}{C}\right]\left\{\frac{1}{[1 + e^2 - 2e\cos(\beta_I)]}[\theta_2^{(2)} - \theta_1^{(2)}]\right\}\frac{1}{r_I} \quad (26)$$

respectively, where the asymptotic forms of the θ integration limits are derived in Appendix AII.2.

In the limit for $r_{Lp} \rightarrow 0$, with $r_{Lp}^2 \geq D^2\sin^2\epsilon(\phi)$ and $r_I > 0$,

$$G_E^{Rf} \rightarrow G^{Rf} = (G_1^{Rf} + G_2^{Rf}) \quad (27)$$

where G^{Rf} is the reflected (indirect) contribution to the incident radiation as predicted by the simplified extense model (SEM).

It is important to remark the fact that the asymptotic expressions of eqs 25 and 26 retain the geometrical features of the elliptical mirror through its eccentricity e and the product of the maximum (a^2/b) and the minimum (b^2/a) radius of curvature of the elliptical cross section through the constant $C = a^2/b^2$.

The expression for the indirect contribution to the local incident radiation inside an elliptical reflecting cavity corresponding to the SEM as the constrained limit of the ESVE model as $r_{Lp} \rightarrow 0$ differs both mathematically and conceptually from the expression for the same contribution based on geometrical optics only. The latter approach stresses the geometry of ray trajectories, stripping them of their diverging character, this being a purely energetic aspect that will always be affected by the local curvature of the elliptical reflecting surface. Models that conceive of the lamp as a line as their starting point have been based on this approach and consequently fail to represent the true contributions of reflected radiation in this type of mirror−lamp setup.

An important limit of eqs 25 and 26 is that of $e \rightarrow 0$. The physical interpretation of this limit is that both reactor and lamp are collinear, corresponding to the case of an annular photoreactor with an external cylindrical reflecting surface. It can be seen that eqs 25 and 26 reduce to a single equation corresponding to the local incident radiation as predicted with the LSSE model for an annular photoreactor with an external cylindrical reflecting surface.

Mathematically, the total incident radiation as predicted by the SEM only requires the closed, explicit eqs 13, 25, 26, and 27 and direct implementation, with no numerical integrations needed.

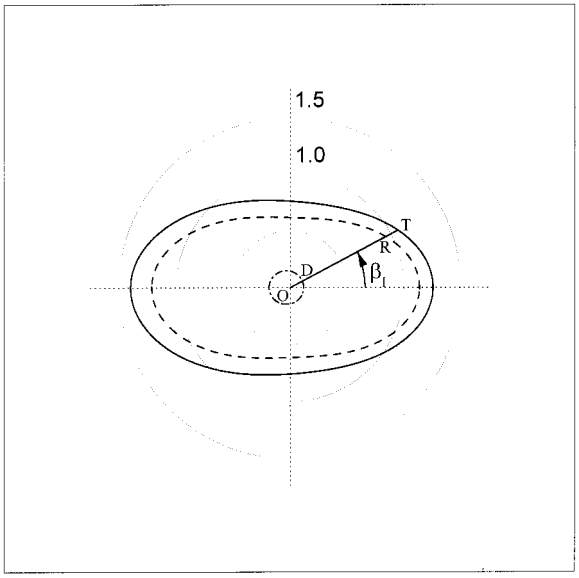

Figure 2. SEM computational results for $r_I = 0.05$ m and $0 \leq \beta_I \leq 2\pi$. Parameters of the elliptical reflector: $a = 0.50$ m and $e = 0.40$. Mirror reflectivity $\Gamma_R = 0.8$. Plotted values are relative to the averaged value G_{Av} over the range of β_I. —, incident radiation g; —·—·—, direct contribution g^D; — — —, indirect radiation g^{Rf}.

III. Incident Radiation Profiles. Predictions Using the Simplified Extense Model

The relative incident radiation, $g = (G/G_{Av})$, as well as the direct, $g^D = (G^D/G_{Av})$, and reflected, $g^{Rf} = (G^{Rf}/G_{Av})$, contributions relative to the average value

$$G_{Av} = \frac{1}{2\pi}\int_0^{2\pi} d\beta_I\, G(\beta_I) \quad (28)$$

where the total incident radiation as a function of β_I, $G(\beta_I)$, has been computed on the basis of eq 13 and eqs 25−27. Each set of calculations has been performed at points β_I on a circumference of radius r_I, centered at the reception focus of the midheight elliptical cross section.

Figure 2 shows computational results based on the SEM for $r_I = 0.05$ m, $0 \leq \beta_I \leq 2\pi$, and the ellipse parameter values $a = 0.50$ m and $e = 0.4$. For every value of β_I, we can identify three collinear radius vectors, each one measuring different contributions to the value of the incident radiation g (full line): (i) the segment $\overline{OD}$ from the origin to the dash-dotted curve measures the direct contribution to the incident radiation, g^D, at the point (z_I, r_I, β_I), as given by eq 14; (ii) the segment $\overline{OR}$ from the origin to the dashed curve represents the reflected (indirect) contribution, g^{Rf}, as given by eqs 25−27; and (iii) the segment $\overline{OT}$ from the origin to the full profile represents the total incident radiation, g, as given by the SEM.

From these results, we can conclude that the indirect radiation clearly dominates over the direct radiation contribution to the incident radiation in the entire range $0 \leq \beta_I \leq 2\pi$. This also explains why the incident radiation has maxima at $\beta_I = 0$ and $\beta_I = \pi$, corresponding to points with local maximum curvature of the mirror and, therefore, of maximum reduction effect on

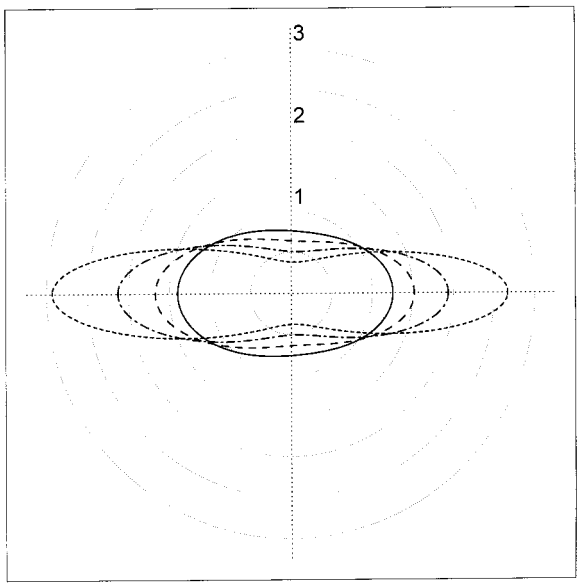

Figure 3. Effect of the ellipse eccentricity, e, on the shape of the incident radiation profile g as predicted using the SEM for $r_I = 0.05$ m and $a = 0.50$ m. Mirror reflectivity $\Gamma_R = 0.8$. Plotted values are relative to the averaged value of G_{Av} over the range of β_I for each eccentricity. —, $e = 0.4$; – – –, $e = 0.5$; —•—•—, $e = 0.6$; - - -, $e = 0.7$.

the beams divergence upon reflection. Minimum values of the total incident radiation G occur when the direction β_I points at segments of the ellipse close to the points with the smallest curvature. In these cases, the minimum of G does not correspond exactly to the directions pointing at the mirror sectors with the smallest curvature mainly because of the additional contribution from the direct radiation. Incidentally, note that the shapes of the direct radiation profiles indicate contributions of this radiation for $-\pi/2 \le \beta_I \le \pi/2$, a situation that might be possible because we are dealing with a diactinic medium.

The effect of the ellipse eccentricity on the shape of the relative incident radiation profile as predicted with the SEM is shown in Figure 3 for $r_I = 0.05$ m, $0 \le \beta_I \le 2\pi$, and the ellipse parameter value $a = 0.5$ m. As the eccentricity increases, the radiation concentration effect due to points on the mirror with local maximum curvature is reinforced. The opposite trend is predicted for the minimum values of the total incident radiation G occurring when radiation is reflected about points with the smallest curvature. On the assumption that this model is a good representation of the actual performance, this result provides an important conclusion for designing these reactors. To achieve uniform irradiation from outside, the ellipse eccentricity must be minimized.

The ratio of the β_I-averaged, direct contribution, G^D_{Av}, to the average total incident radiation, G_{Av}, is shown in Figure 4 for $a = 0.5$ m, $e = 0.4$, and $\Gamma_R = 0.8$, as a function of the dimensionless distance from the reception focal axis to the incidence point, r_I/a. As the incidence point is located farther away from the reception focal axis, the importance of the direct radiation contribution increases when compared to the average total incident radiation. Despite this trend predicted by the SEM, the direct radiation contribution is never larger than 15% of the total incident radiation for the considered setup and for reasonable values of r_I/a, as is also the case with the ESVE.[31] Once more, we can draw some additional design conditions: to increase uniformity in the radiation field for a given reactor radius, the elliptical reflector cannot be small (a must be large).

IV. Comparison with the Extense Source Model

The ESVE and the SEM were compared under similar conditions. In Figure 5, results corresponding to the set of parameter values $a = 0.5$ m, $e = 0.4$, and $(r_I/a) = 0.1$ are shown for both the SEM and the ESVE. In the case of the ESVE, values of $(r_{Lp}/a) = 0.01$, 0.02, and 0.04 have been chosen. The results show that the incident radiation profiles obtained with the SEM (full profile) agree quite well with those obtained with the ESVE for $(r_{Lp}/a) = 0.01$ and $(r_{Lp}/a) = 0.02$. Although larger β_I-dependent errors can be observed for $(r_{Lp}/a) = 0.04$, the β_I-averaged values show a much better agreement. Let us look at these values.

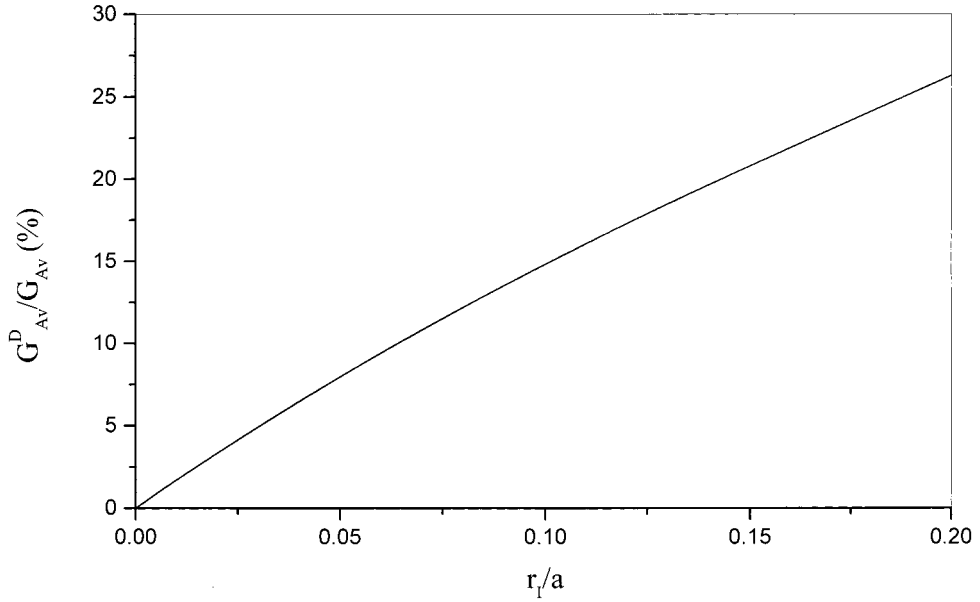

Figure 4. SEM predicted ratio of the β_I-averaged, direct contribution G^D_{Av} to the averaged total incident radiation G_{Av} for $a = 0.50$ m, $e = 0.4$, and $\Gamma_R = 0.8$ vs the dimensionless distance from the reception focal axis to the incidence point, r_I/a.

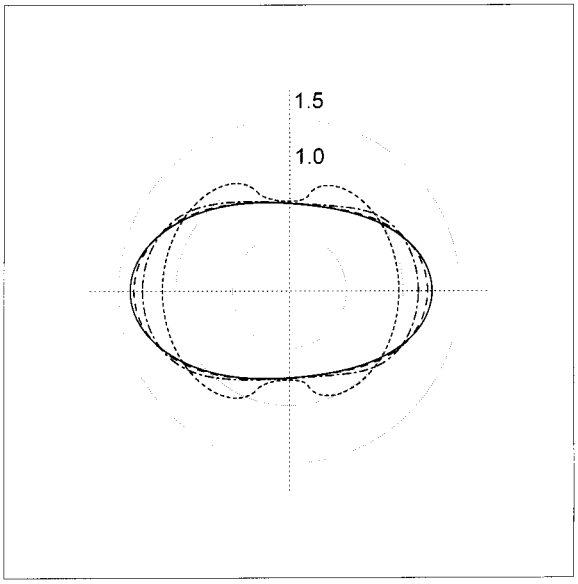

Figure 5. Comparison of SEM (—) and ESVE computed g values for several lamp radii r_{Lp} and $r_I = 0.05$ m. Parameters of the elliptical reflector are $a = 0.50$ m and $e = 0.40$. Mirror reflectivity $\Gamma_R = 0.8$. Plotted values are relative to the averaged value G_{Av} over the range of β_I. – – –, ESVE for $r_{Lp}/a = 0.01$; —·—·—, ESVE for $r_{Lp}/a = 0.02$; - - -, ESVE for $r_{Lp}/a = 0.04$.

From the definition of the β_I-averaged total incident radiation in eq 28, we can readily derive the following expression:

$$G_{Av} = \frac{P_L}{2\pi}\int_0^{2\pi} d\beta_I \frac{G(\beta_I)}{P_L} \tag{29}$$

On the basis of eqs 13, 25, and 26, we can conclude that the integral factor in eq 29 depends only on the geometry of the setup and on effective reflection and transmission factors, being independent of the lamp output power. In a similar manner, for the ESVE, we have

$$G_{E,Av} = \frac{P_V}{2\pi}\int_0^{2\pi} d\beta_I \frac{G_E(\beta_I)}{P_V} \tag{30}$$

For the purpose of model comparison, a function Error-(%) can be defined

$$\text{Error}(\%) = \left[1 - \left(\frac{G_{Av}}{G_{E,Av}}\right)\right] \times 100 \tag{31}$$

From eq 11, and for equal lamp output power, the function Error(%) can also be written

$$\text{Error}(\%) = \left[1 - (\pi r_{Lp}^2)\left(\frac{\int_0^{2\pi} d\beta_I \frac{G(\beta_I)}{P_L}}{\int_0^{2\pi} d\beta_I \frac{G_E(\beta_I)}{P_V}}\right)\right] \times 100 \tag{32}$$

Figure 6 shows the function Error(%) vs (r_{Lp}/a) for $a = 0.5$ m; $e = 0.4$; and values of $(r_I/a) = 0.025$, 0.050, 0.100, and 0.200. The value of Error(%) is always below 12% for the range of values of (r_{Lp}/a) and (r_I/a) chosen and drops dramatically for $(r_{Lp}/a) < 0.020$. The accuracy of the SEM also increases with the ratio (r_I/r_{Lp}).

For the set of parameters $a = 0.5$ m, $e = 0.6$, and $(r_I/a) = 0.1$, Figure 7 clearly pictures how the incident radiation profiles predicted with the ESVE for different (r_{Lp}/a) values continuously tend to that predicted with the SEM (full profile) as $(r_{Lp}/a) \rightarrow 0$. However, note that the ESVE model indicates that the larger the lamp radius is, the more uniform is the radiation field for a given radial position in the reactor. Although not derived from the SEM, this is again valuable design information.

V. Conclusions

The extense source models (ESM) have been widely considered as the best available mathematical representation so far for predicting photoreactor radiation field properties, its main drawback arising from the difficulties of its numerical implementation. In the

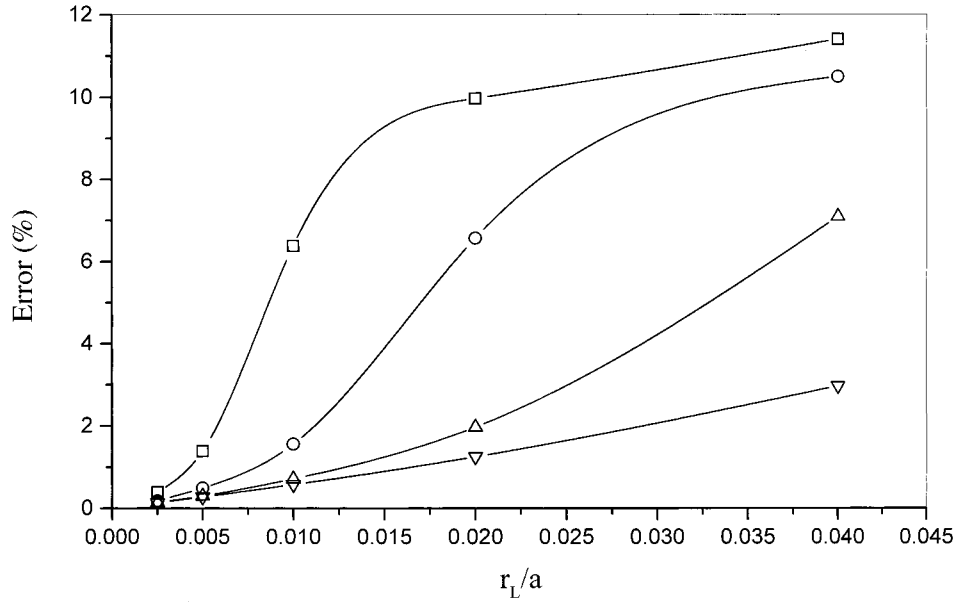

Figure 6. Comparison of SEM and ESVE performances for several distances from the reception focal axis to the incidence point, r_I. Parameters of the elliptical reflector are $a = 0.50$ m and $e = 0.40$. Mirror reflectivity $\Gamma_R = 0.8$. Plotted function Error(%) as defined in eq 32. □, $r_I/a = 0.025$; ○, $r_I/a = 0.050$; △, $r_I/a = 0.100$; ▽, $r_I/a = 0.200$.

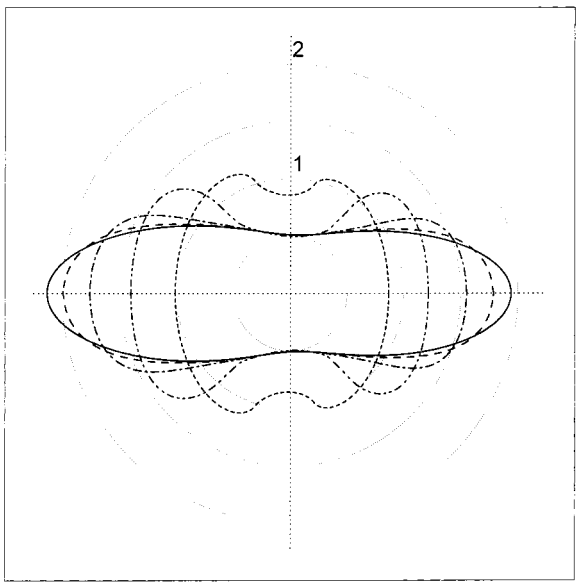

Figure 7. Comparison of SEM (—) and ESVE computed g values for several lamp radii r_{Lp} and $r_I = 0.05$m. Parameters of the elliptical reflector are $a = 0.50$ m and $e = 0.40$. Mirror reflectivity $\Gamma_R = 0.8$. Plotted values are relative to the averaged value G_{Av} over the range of β_I. — — —, ESVE for $r_{Lp}/a = 0.005$; —·—·—, ESVE for $r_{Lp}/a = 0.010$; —··—··—, ESVE for $r_{Lp}/a = 0.020$; - - -, ESVE for $r_{Lp}/a = 0.040$.

present work, a simplified extense model is proposed that takes the ESVE as the starting point. The leading notion is that of considering the radiation field properties predicted with the SEM as the respective asymptotic mathematical expressions given by the ESVE as the lamp radius tends to zero.

This process is conceptually different from those considering a line source with spherical emission, which already is the result of a previous physical limiting process as the starting model element for computing direct and indirect incident radiation at a given point in the reaction space resorting to geometrical optics to trace ray trajectories. By operating in this manner, changes in the divergence of the energy beams when reflected on the curved mirror are definitely lost, hampering the ability of the LSM to predict indirect radiation contributions with the desired accuracy.

The SEM is mathematically simple to apply. The incident radiation profiles for nonparticipating media are given as closed, analytical expressions that are amenable to direct calculation and very easy to implement in a computer program. Moreover, for direct radiation contributions, it provides the same degree of simplicity that has been found in the LSSE model. Despite its simplicity, the SEM retains the relevant features of the ESVE, specifically those related to the indirect radiation contribution.

The results show that the incident radiation profiles obtained with the SEM agree quite well with those obtained with the ESVE for lamp radii smaller than 0.01 m. Although larger β_I-dependent errors can be observed for thicker lamps, the β_I-averaged values predicted with the ESVE and SEM are in excellent agreement. For $a = 0.5$ m, the value of Error(%) is always below 12% for the range of values of (r_{Lp}/a) and (r_I/a) tested and drops dramatically for $(r_{Lp}/a) < 0.020$. The accuracy of the SEM also increases with the ratio (r_I/r_{Lp}).

Acknowledgment

This work was supported by the Argentine National Research Council (CONICET) and the Universidad Nacional del Litoral. The authors gratefully acknowledge financial support from the National Agency for the Promotion of Science and Technology (ANPCyT).

Appendix AI

AI.1. Equations of the ESVE Model for the Prediction of the Direct Contribution to the Incident Radiation. The expression for the direct incident radiation as predicted with the ESVE model in a diactinic medium is

$$G_E^D = P_V \Psi_R \int_\theta \int_\phi \int_\rho d\theta \, d\phi \, d\rho \sin\theta \qquad \text{(AI.1)}$$

where the value of P_V is given by

$$P_V = \frac{E_{Lp}}{4\pi^2 L_{Lp} r_{Lp}^2} \qquad \text{(AI.2)}$$

From eq AI.2, it can be seen that the entire lamp dimensions, as well as its output power, are included in the definition of P_V. E_{Lp} is the monochromatic emission, usually expressed in terms of einstein s^{-1}.

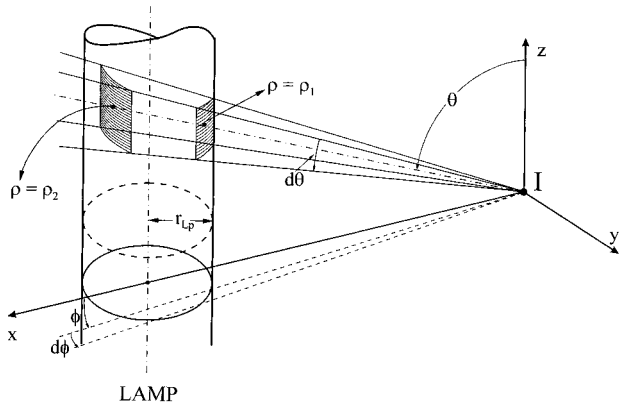

Figure AI.1. ESVE model. Parameters and variables associated with the direct radiation contribution to the incident radiation at $I(z_I, r_I, \beta_I)$. Adapted from Irazoqui et al.[7]

As shown in Figure AI.1, the limits of the ρ integration in eq AI.1 are

$$\rho_{1,2}(\theta,\phi) = \frac{\Delta \cos\phi \mp [r_{Lp}^2 - \Delta^2 \sin^2\phi]^{1/2}}{\sin\theta} \qquad \text{(AI.3)}$$

respectively, where from Figure AI.2

$$\Delta = [(2c + r_I \cos\beta_I)^2 + r_I^2 \sin^2\beta_I]^{1/2} \qquad \text{(AI.4)}$$

The limits of the θ and ϕ integrations are

$$\theta_1(\phi) = \tan^{-1}\left[\frac{\Delta\cos\phi - [r_{Lp}^2 - \Delta^2\sin^2\phi]^{1/2}}{{}^1/_2(L_{Rf} - L_{Lp}) - z_I}\right] \qquad \text{(AI.5)}$$

$$\theta_2(\phi) = \pi - \tan^{-1}\left[\frac{\Delta\cos\phi - [r_{Lp}^2 - \Delta^2\sin^2\phi]^{1/2}}{z_I - {}^1/_2(L_{Rf} - L_{Lp})}\right] \qquad \text{(AI.6)}$$

and

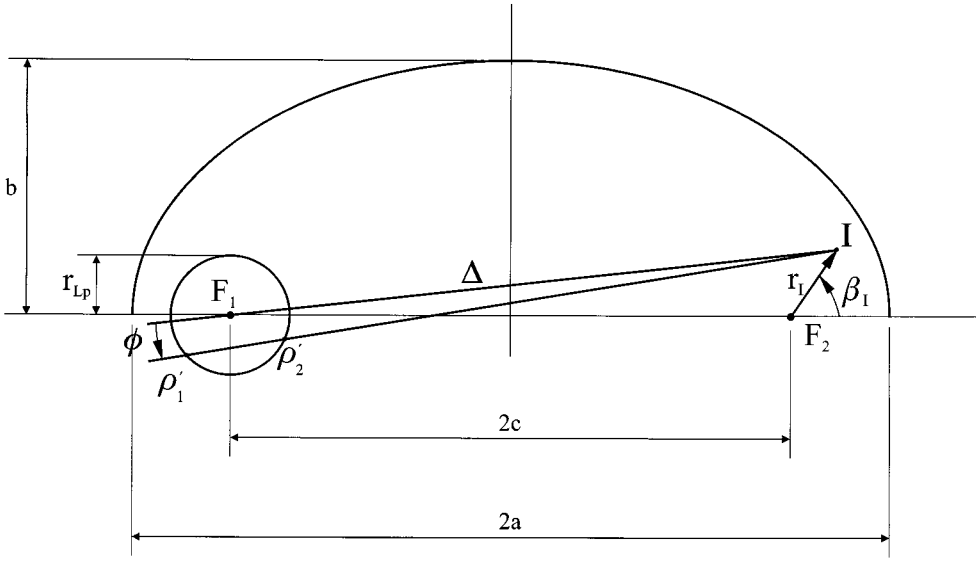

Figure AI.2. ESVE model. Projections on the cross section, as well as parameters and variables associated with the direct radiation contribution to the incident radiation at $I(z_I, r_I, \beta_I)$.

$$\phi_2 = \sin^{-1}\left(\frac{r_{Lp}}{\Delta}\right) \tag{AI.7}$$

$$\phi_1 = -\phi_2 \tag{AI.8}$$

respectively, as can be concluded from Figures 1, AI.1, and AI.3.

AI.2. The Integral in Equation 11. The integral on the rhs of eq 11 is analytical and can be substituted by its indefinite expression found in standard mathematical tables, i.e.,

$$\int dx\,(A + Bx^2)^{1/2} = \frac{x}{2}(A + Bx^2)^{1/2} - \frac{A}{2(-B)^{1/2}} \sin^{-1}\frac{Bx}{(-AB)^{1/2}} \tag{AI.9}$$

In the case of direct radiation, by identifying $x = \phi$ and

$$A = r_{Lp}^2 \tag{AI.10}$$

$$B = -\Delta^2 \tag{AI.11}$$

we obtain the definite integral expression

$$\int_{\phi_1}^{\phi_2} d\phi\,[r_{Lp}^2 - \Delta^2\phi^2]^{1/2} = \left\{\frac{\phi}{2}[r_{Lp}^2 - \Delta^2\phi^2]^{1/2}\right\}_{\phi_1}^{\phi_2} - \frac{r_{Lp}^2}{2\Delta}\left[\sin^{-1}\left(-\frac{\Delta}{r_{Lp}}\phi\right)\right]_{\phi_1}^{\phi_2} \tag{AI.12}$$

After eqs 7 and 8 are substituted into eq AI.12 and the result thus obtained is used in eq 11, we finally arrive at the limit form

$$G_E^D \rightarrow 2P_V\Psi_R[\theta_2 - \theta_1]\left(-\frac{r_{Lp}^2}{2\Delta}\right)[\sin^{-1}(-1) - \sin^{-1}(1)] \tag{AI.13}$$

as $r_{Lp} \rightarrow 0$. Therefore,

$$G_E^D \rightarrow (\pi P_V r_{Lp}^2)\Psi_R\frac{[\theta_2 - \theta_1]}{\Delta} \tag{AI.14}$$

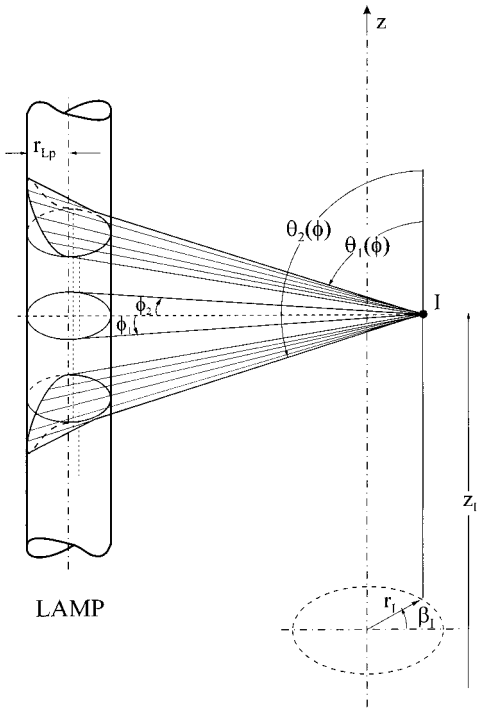

Figure AI.3. ESVE model. Limits of integration of the variables θ and ϕ associated with the direct radiation contribution to the incident radiation at $I(z_I, r_I, \beta_I)$. Adapted from Irazoqui et al.[7]

is the limit form of G_E^D when $r_{Lp} \rightarrow 0$, always satisfying the constraint that $(r_{Lp}^2 - \Delta^2 \sin^2\phi) \geq 0$. From eq AI.2, it can be also concluded that the product $(\pi P_V r_{Lp}^2)$ remains a finite quantity in the limiting process.

Appendix AII

AII.1. Equations of the ESVE Model for the Prediction of the Indirect Contribution to the Incident Radiation. In eq 15,

$$D = a\frac{[1 + e^2 + 2e\cos\alpha]}{[1 + e\cos\alpha]} \tag{AII.1}$$

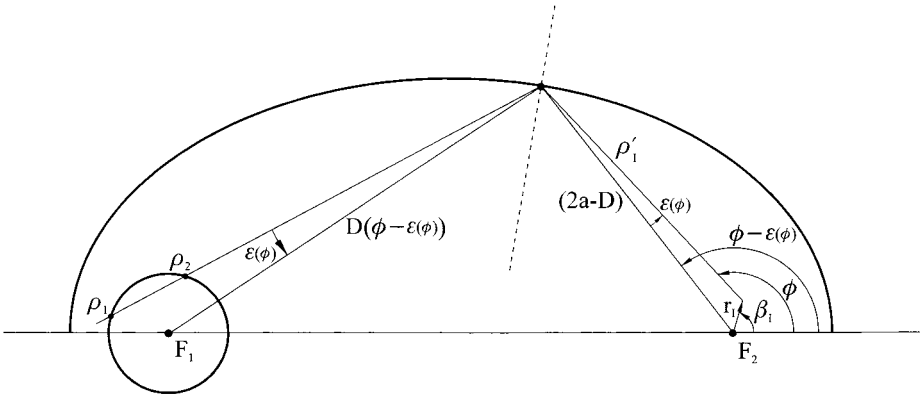

Figure AII.1. ESVE model. Projections on the cross section, as well as parameters and variables associated with the reflected radiation contribution to the incident radiation at $I(z_I, r_I, \beta_I)$.

where a and e are parameters of the elliptical reflector and α is defined in Table 1.

Table 1. Parameter α in Equation AII.1 as a Function of β_I, ϕ, and $\epsilon(\phi)$[a]

$\phi \geq \beta_I$	$\phi - \beta_I \leq \pi$	$\alpha = \phi - \epsilon$
	$\phi - \beta_I > \pi$	$\alpha = \phi + \epsilon$
$\phi < \beta_I$	$\beta_I - \phi \leq \pi$	$\alpha = \phi + \epsilon$
	$\beta_I - \phi > \pi$	$\alpha = \phi - \epsilon$

[a] For all entries, $\epsilon \geq 0$.

From the relationship

$$[2a - D(\phi)] \sin \epsilon = r_I |\sin(\phi - \beta_I)| \quad \text{(AII.2)}$$

derived from Figure AII.1, we readily obtain

$$\sin \epsilon = \frac{r_I |\sin(\phi - \beta_I)|}{[2a - D(\phi)]} \quad \text{(AII.3)}$$

For given (r_I, β_I, ϕ) values, the set of eqs AII.1, AII.2, and AII.3 can be solved.

The limits of the θ integration are

$$\theta_1(\phi) = \tan^{-1}\left[\frac{\rho'_I + D\cos\epsilon - [r_{Lp}^2 - D^2 \sin^2 \epsilon]^{1/2}}{{}^1/_2(L_{Rf} + L_{Lp}) - z_I}\right] \quad \text{(AII.4)}$$

and

$$\theta_2(\phi) = \pi - \tan^{-1}\left[\frac{\rho'_I + D\cos\epsilon - [r_{Lp}^2 - D^2 \sin^2 \epsilon]^{1/2}}{z_I - {}^1/_2(L_{Rf} - L_{Lp})}\right] \quad \text{(AII.5)}$$

where

$$\rho'_I = -r_I \cos(\phi - \beta_I) + [(2a - D)^2 - r_I^2 \sin^2(\phi - \beta_I)]^{1/2} \quad \text{(AII.6)}$$

From Figure AII.1, we also conclude that the set of ϕ integration limits is obtained by solving the following implicit equation:

$$[D(\phi_{limit} - \epsilon(\phi_{limit}))]^2 \sin^2\epsilon(\phi_{limit}) = r_{Lp}^2 \quad \text{(AII.7)}$$

AII.2. Derivation of the Asymptotic Form of the θ Integration Limits in Equations 26 and 27. When eqs 24 and 25 are used in eq 15, two contributions to the local indirect incident radiation can be identified, each one having the general form of eq AI.9. With the definitions

$$A_1 \equiv 1 \quad \text{(AII.8)}$$

$$B_1 \equiv -C^2[1 + e^2 + 2e\cos(\beta_I)]^2\left(\frac{r_I}{r_{Lp}}\right)^2 \quad \text{(AII.9)}$$

$$A_2 \equiv 1 \quad \text{(AII.10)}$$

$$B_2 \equiv -C^2[1 + e^2 - 2e\cos(\beta_I)]^2\left(\frac{r_I}{r_{Lp}}\right)^2 \quad \text{(AII.11)}$$

the asymptotic forms given by eqs 24 and 25 can be written as

$$r_{Lp}^2 - D^2(\phi)\sin^2\epsilon \approx r_{Lp}^2[A_1 + B_1(\phi - \beta_I)^2] \quad \text{(AII.12)}$$

and

$$r_{Lp}^2 - D^2(\phi)\sin^2\epsilon \approx r_{Lp}^2[A_2 + B_2(\phi - \beta_I - \pi)^2] \quad \text{(AII.13)}$$

respectively.

In the limit for $r_{Lp} \to 0$, with $r_{Lp}^2 \geq D^2 \sin^2 \epsilon(\phi)$ and $r_I > 0$, there are two illuminated wedge-shaped zones converging to points with different z_I but sharing the same pair of values (r_I, β_I). To each of these two zones corresponds a pair of ϕ integration limits, ($\phi_I^{(1)} < \beta_I < \phi_2^{(1)}$) and ($\phi_I^{(2)} < \beta_I + \pi < \phi_2^{(2)}$), that can be obtained from the condition that the lhs of eqs 24 and 25 be zero. The result is

$$\xi_{2,1}^{(1)} = \phi_{2,1}^{(1)} - \beta_I = \pm\frac{1}{C}\left(\frac{r_{Lp}}{r_I}\right)\frac{1}{[1 + e^2 + 2e\cos(\beta_I)]} \quad \text{for } \phi_I^{(1)} < \beta_I < \phi_2^{(1)} \quad \text{(AII.14)}$$

$$\xi_{2,1}^{(2)} = \phi_{2,1}^{(2)} - (\beta_I + \pi) = \pm\frac{1}{C}\left(\frac{r_{Lp}}{r_I}\right)\frac{1}{[1 + e^2 - 2e\cos(\beta_I)]} \quad \text{for } \phi_I^{(2)} < \beta_I + \pi < \phi_2^{(2)} \quad \text{(AII.15)}$$

From eqs AII.4, AII.5, and AII.6, it can be concluded that the asymptotic forms of the θ integration limits are

$$\theta_1^{(1)} \approx \tan^{-1}\left[\frac{2a - r_I}{{}^1/_2(L_{Rf} + L_{Lp}) - z_I}\right]$$

$$\text{for } \phi_I^{(1)} < \beta_I < \phi_2^{(1)} \quad \text{(AII.16)}$$

$$\theta_2^{(1)} \approx \pi - \tan^{-1}\left[\frac{2a - r_I}{z_I - {}^1/_2(L_{Rf} - L_{Lp})}\right]$$

and

$$\theta_1^{(2)} \approx \tan^{-1}\left[\frac{2a + r_I}{{}^1/_2(L_{Rf} + L_{Lp}) - z_I}\right]$$

$$\text{for } \phi_I^{(2)} < \beta_I + \pi < \phi_2^{(2)} \quad \text{(AII.17)}$$

$$\theta_2^{(2)} \approx \pi - \tan^{-1}\left[\frac{2a + r_I}{z_I - {}^1/_2(L_{Rf} - L_{Lp})}\right]$$

respectively.

Substituting the asymptotic forms thus obtained into eqs 24 and 25, we can identify the two contributions to the indirect incident radiation, corresponding to the illuminated wedge-shaped zones converging to points with different z_I but sharing the same pair of values (r_I, β_I). The contribution corresponding to the integration interval $\phi_I^{(1)} < \beta_I < \phi_2^{(1)}$ is

$$G_1^{Rf} = 2P_V\Psi_R\Gamma_{Rf}r_{Lp}\{[\theta_2^{(1)} - \theta_1^{(1)}]\int_{\zeta_1^{(1)}}^{\zeta_2^{(1)}} d\zeta[A_1 + B_1\zeta^2]^{1/2}\} \quad \text{(AII.18)}$$

while the remaining contribution, corresponding to the interval $\phi_I^{(2)} < \beta_I + \pi < \phi_2^{(2)}$, is

$$G_2^{Rf} = 2P_V\Psi_R\Gamma_{Rf}r_{Lp}\{[\theta_2^{(2)} - \theta_1^{(2)}]\int_{\zeta_1^{(2)}}^{\zeta_2^{(2)}} d\zeta[A_2 + B_2\zeta^2]^{1/2}\} \quad \text{(AII.19)}$$

Equations AII.18 and AII.19 have the general form of eq AI.9; therefore, they can be integrated analytically.

Notation

a = ellipse parameter, see Figure 3
b = ellipse parameter, see Figure 3
c = ellipse parameter, see Figure 3
C = dimensionless constant, defined by eq 32
e = ellipse eccentricity, dimensionless
E = monochromatic emission, einsteins s^{-1}
G = incident radiation, einsteins s^{-1} m^{-2}
g = relative incident radiation, dimensionless
I = specific intensity, einsteins s^{-1} m^{-2} sr^{-1}
L = length, m
P_L = lamp constant in the LSSE model, einsteins m^{-1} s^{-1}
P_V = characteristic property of the lamp emission, defined by eq 4, einstein s^{-1} m^{-3} sr^{-1}
r_{Lp} = lamp arc radius, m
r_I = distance from the reception focal axis to the incidence point, m
z_I = coordinate of the incidence point, m

Subscripts

E = property calculated with the ESVE model
Lp = lamp
Rf = reflector

Superscripts

Av = β_I-averaged property
D = direct
Rf = reflected

Greek Letters

Ω = solid angle, sr
Γ_R = mirror reflection coefficient, dimensionless
Ψ_R = transmission coefficient, dimensionless

Literature Cited

(1) Gaertner, R. E.; Kent, J. A. Conversion in a Continuous Photochemical Reactor. *Ind. Eng. Chem.* **1958**, *50*, 1223.

(2) Harris, P. R.; Dranoff, J. S. A Study of Perfectly Mixed Photochemical Reactors. *AIChE J.* **1965**, *11*, 497.

(3) Romero, R. L.; Alfano, O. M.; Marchetti, J. L.; Cassano, A. E. Modeling and Parametric Sensitivity of an Annular Photoreactor with Complex Kinetics. *Chem. Eng. Sci.* **1983**, *38*, 1593.

(4) Jacob, S. M.; Dranoff, J. S. Radial Scale-up of Perfectly Mixed Photochemical Reactors. *Chem. Eng. Prog. Symp. Ser.* **1966**, *62*, 47.

(5) Jacob, S. M.; Dranoff, J. S. Design and Analysis of Perfectly Mixed Photochemical Reactors. *Chem. Eng. Prog. Symp. Ser.* **1968**, *64*, 54.

(6) Alfano, O. M.; Romero, R. L.; Cassano, A. E. Radiation Field Modelling in Photoreactors I. Homogeneous Media. *Chem. Eng. Sci.* **1986**, *41*, 421.

(7) Irazoqui, H. A.; Cerdá, J.; Cassano, A. E. Radiation Profiles in an Empty Annular Photoreactor with a Source of Finite Spatial Dimensions. *AIChE J.* **1973**, *19*, 460.

(8) Stramigioli, C.; Santarelli, F.; Foraboschi, F. P. Photosensitized Reactions in an Annular Photoreactor. *Ing. Chim. Ital.* **1975**, *11*, 143.

(9) Stramigioli, C.; Santarelli, F.; Foraboschi, F. P. Photosensitized Reactions in an Annular Continuous Photoreactor, *Appl. Sci. Res.* **1977**, *33*, 23.

(10) De Bernardez, E. R.; Cassano, A. E. A Priori Design of a Continuous Annular Photochemical Reactor. Experimental Validation for Simple Reactions. *J. of Photochemistry* **1985**, *30*, 285.

(11) De Bernardez, E. R.; Cassano, A. E. Methodology for an Optimal Design of a Photoreactor. Application to Methane Chloroderivatives Production. *Ind. Eng. Chem. Process Des. Dev.* **1986**, *25*, 601.

(12) Clariá, M. A.; Irazoqui, H. A.; Cassano, A. E. Modelling and Experimental Validation of the Radiation Field Inside an Elliptical Photoreactor. *The Chem. Eng. J.* **1986**, *33*, 119.

(13) Clariá, M. A.; Irazoqui, H. A.; Cassano, A. E. A Priori Design of a Photoreactor for the Chlorination of Ethane. *AIChE J.* **1988**, *34*, 355.

(14) Alfano, O. M.; Romero, R. L.; Cassano, A. E. A Cylindrical Photoreactor Irradiated from the Bottom. I. Radiation Flux Density Generated by a Tubular Source with a Parabolic Reflector. *Chem. Eng. Sci.* **1985**, *40*, 2119.

(15) Alfano, O. M.; Romero, R. L.; Cassano, A. E. A Cylindrical Photoreactor Irradiated from the Bottom. II. Model for the Local Volumetric Rate of Energy Absorption with Polychromatic Radiation and their Evaluation. *Chem. Eng. Sci.* **1986**, *41*, 1155.

(16) Alfano, O. M.; Romero, R. L.; Negro, A. C.; Cassano, A. E. A Cylindrical Photoreactor Irradiated from the Bottom. III. Measurement of Absolute Values of the Local Volumetric Rate of Energy Absorption. Experiments with Polychromatic Radiation. *Chem. Eng. Sci.* **1986**, *41*, 1163.

(17) Alfano, O. M.; Cassano, A. E. Modelling of a Gas−liquid Tank Photoreactor Irradiated from the Bottom. I. Theory. *Ind. Eng. Chem. Res.* **1988**, *27*, 1087.

(18) Alfano, O. M.; Cassano, A. E. Modelling of a Gas−liquid Tank Photoreactor Irradiated from the Bottom. II. Experiments. *Ind. Eng. Chem. Res.* **1988**, *27*, 1095.

(19) Alfano, O. M.; Vicente, M.; Esplugas, S.; Cassano, A. E. Radiation Field Inside a Tubular Multilamp Reactor for Water and Wastewater Treatment. *Ind. Eng. Chem. Res.* **1990**, *29*, 1270.

(20) Esplugas, S.; Vicente, M.; Alfano, O. M.; Cassano, A. E. Effect of the Reflector Shape on the Performance of Multilamp Photoreactors Applied to Pollution Abatement. *Ind. Eng. Chem. Res.* **1990**, *29*, 1283.

(21) Vicente, M.; Alfano, O. M.; Esplugas, S.; Cassano, A. E. Design and Experimental Verification of a Tubular Multilamp Reactor for Water and Wastewater Treatment. *Ind. Eng. Chem. Res.* **1990**, *29*, 1278.

(22) Cabrera, M. I.; Alfano, O. M.; Cassano, A. E. Product Yield and Selectivity Studies in Photoreactor Design. Theory and Experiments for the Chlorination of Methane. *Chem. Eng. Sci.* **1990**, *45*, 2439.

(23) Cabrera, M. I.; Alfano, O. M.; Cassano, A. E. Selectivity Studies in the Photochlorination of Methane I: Reactor Model and Kinetic Studies in a Nonisothermal, Polychromatic Environment. *Chem. Eng. Commun.* **1991**, *107*, 95.

(24) Cabrera, M. I.; Alfano, O. M.; Cassano, A. E. Selectivity Studies in the Photochlorination of Methane II: Effect of the Radiation Source Output Power and Output Spectral Distribution. *Chem. Eng. Commun.* **1991**, *107*, 123.

(25) Cabrera, M. I.; Alfano, O. M.; Cassano, A. E. Nonisothermal Photochlorination of Methyl Chloride in the Liquid Phase. *AIChE J.* **1991**, *37*, 1471.

(26) Tymoschuck, A. R.; Alfano, O. M.; Cassano, A. E. The Multitubular Photoreactor I: Radiation Field Distribution in Constant Absorption Reactors. *Ind. Eng. Chem. Res.* **1993**, *32*, 1328.

(27) Tymoschuck, A. R.; Negro, A. C.; Alfano, O. M.; Cassano, A. E. The Multitubular Photoreactor II: Reactor Modeling and Experimental Verification. *Ind. Eng. Chem. Res.* **1993**, *32*, 1342.

(28) Pascuali, M.; Santarelli, F.; Porter, J. F.; Yue, P. L. Radiative Transfer in Photocatalytic Systems. *AICHE J.* **1996**, *42*, 532.

(29) Li Puma, G.; Yue, P. L. A Laminar Falling Film Slurry Photocatalytic Reactor. Part I. Model Development. *Chem. Eng. Sci.* **1998**, *53*, 2993.

(30) Cerdá, J.; Marchetti, J. L.; Cassano, A. E. Radiation Efficiencies in Elliptical Photoreactors. *Lat. Am. J. Heat Mass Transfer* **1977**, *1*, 33.

(31) *Cleaning up with the Sun*. Report SERI/TP-253-3687. Solar Energy Research Institute: Golden, CO, 1990.

(32) Link, H. F.; Turchi, C. S. *Cost and Performance Projections for Solar Energy Water Detoxification Systems*; ASME International Solar Energy Meeting Reno, Nevada, 1991.

(33) Turchi, C. S.; Link, H. F. *Relative Cost of Photons from Solar or Electric Sources for Photocatalytic Water Detoxification*. International Solar Energy Society 1991 Solar World Congress, Denver, Colorado, 1991.

(34) Dillert, R.; Cassano, A. E.; Goslich, R.; Bahnemann, D. Large Scale Studies in Solar Catalytic Wastewater Treatment. *Catal. Today* **1999**, *54*, 267.

(35) Alfano, O. M.; Bahnemann, D.; Cassano, A. E.; Dillert, R.; Goslich, R. Photocatalysis in Water Environments Using Artificial and Solar Light. *Catal. Today* **2000**, *58*, 199.

(36) Ozisik, M. N. *Radiative Transfer and Interactions with Conduction and Convection*; Wiley: New York, 1973; Chapter 1, p 34.

(37) Cerdá, J.; Irazoqui, H. A.; Cassano, A. E. Radiation Fields Inside an Elliptical Photoreactor with a Source of Finite Spatial Dimensions. *AIChE J.* **1973**, *19*, 963.

Received for review November 3, 1999
Revised manuscript received July 11, 2000
Accepted August 10, 2000

IE9907876